

解説

**An Isothermal Titration Calorimetric Study of  
the Antigen-Antibody Interaction: The Affinity Maturation of  
Anti-4-Hydroxy-3-Nitrophenylacetyl Mouse Monoclonal Antibody**

Hidetaka Torigoe

(Received November 2, 2000; Accepted November 15, 2000)

To understand the mechanism of affinity maturation, the antigen-antibody interactions between 4-hydroxy-3-nitrophenylacetyl caproic acid (NP-Cap) and the Fab fragments of three anti-4-hydroxy-3-nitrophenylacetyl (NP) antibodies, N1G9, 3B44, and 3B62, were examined by isothermal titration calorimetry. The analyses revealed that all of these interactions were mainly driven by negative changes in enthalpy. The enthalpy changes decreased linearly with temperature in the range of 25 ~ 45 °C, producing negative changes in heat capacity. On the basis of the dependency of binding constants on the sodium chloride concentration, it was shown that, during the affinity maturation of the anti-NP antibody, the electrostatic effect did not significantly contribute to the increase in the binding affinity. It was also found that, as the logarithm of the binding constants increased during the affinity maturation of the anti-NP antibody, the magnitudes of the corresponding enthalpy, heat capacity, and unitary entropy changes increased almost linearly. On the basis of this correlation, it is concluded that, during the affinity maturation of the anti-NP antibody, a better surface complementarity is attained in the specific complex to obtain a higher binding affinity.

### 1. Introduction

In affinity maturation of the immune response, the average affinity of the immunized serum generally increases with time after immunization.<sup>1)</sup> To investigate the relationship between the primary sequence diversity of antibodies and the progressive change in binding affinity, extensive analyses of antibodies have been carried out by using several haptens, 4-hydroxy-3-nitrophenylacetyl (NP),<sup>2-5)</sup> p-azophenylarsonate,<sup>6)</sup> phosphorylcholine,<sup>7)</sup> and 2-phenyl-5-oxazolone.<sup>8)</sup>

A series of anti-NP mouse monoclonal IgG antibodies used in the present study were produced by the immune response of C57BL/6 mice against NP coupled

to T cell dependent carrier, chicken gamma globulin.<sup>9, 10)</sup> The variable regions of the primary response anti-NP antibodies show low affinity for NP and carry few, if any, somatic mutations,<sup>2,4)</sup> whereas those of the secondary response anti-NP antibodies usually exhibit increased affinity for NP and are somatically mutated.<sup>5)</sup> The secondary response antibodies are divided into two groups by carrying or lacking a somatic Trp → Leu exchange at position 33 in the variable region of the heavy chain.<sup>11, 12)</sup> In the present study N1G9, a primary response anti-NP antibody, was compared with 3B44 and 3B62, which are secondary response anti-NP antibodies with and without Trp → Leu exchange, respectively.

Thermodynamic aspect of antigen-antibody

---

The abbreviations used are:  $\Delta C_p$ , heat capacity change; Fab, antigen binding fragment composed of the light chain and the N-terminal half of the heavy chain;  $\Delta G_u$ , unitary Gibbs free energy change; ITC, isothermal titration calorimetry;  $K_a$ , binding constant; NMR, nuclear magnetic resonance; NP, 4-hydroxy-3-nitrophenylacetyl; NP-Cap, 4-hydroxy-3-nitrophenylacetyl caproic acid;  $\Delta S_u$ , unitary entropy change.

© 2001 The Japan Society of Calorimetry and Thermal Analysis.

association is essential to understand the mechanism of the high affinity and specificity of antigen-antibody interaction. Thermodynamic parameters, such as Gibbs free energy change,  $\Delta G$ , enthalpy change,  $\Delta H$ , entropy change,  $\Delta S$ , and heat capacity change,  $\Delta C_p$ , can provide useful information to identify fundamental forces involved in the antigen-antibody interaction. For instance, the magnitude of  $\Delta C_p$  is usually related to the contribution of the hydrophobic effect to molecular association.<sup>13-16)</sup>

With the recent improvement in the sensitivity and reliability of the calorimeter,<sup>17,18)</sup> isothermal titration calorimetry (ITC) has become a powerful tool for the direct measurement of thermodynamic parameters in various biological interactions, such as protein-protein interactions,<sup>19-22)</sup> oligosaccharide-lectin associations<sup>23-25)</sup> and ligand binding to proteins.<sup>26,27)</sup> Recently this method has been applied to the quantitative thermodynamic analyses of antibody binding to various types of antigens, *e.g.*, haptens,<sup>28-31)</sup> oligosaccharides<sup>32-34)</sup> and proteins.<sup>35-44)</sup> However, no calorimetric studies have been reported on the antigen-antibody interaction in the affinity maturation.

In the present study, the antigen-antibody associations in the affinity maturation were analyzed by ITC. The interactions between 4-hydroxy-3-nitrophenylacetyl caproic acid (NP-Cap) antigen and the Fab fragments of three anti-NP antibodies, N1G9, 3B44, and 3B62, were examined. On the basis of the obtained thermodynamic data, it was found that the binding constants,  $K_a$ , for NP-Cap correlated with each of the  $\Delta H$ ,  $\Delta C_p$ , and  $\Delta S_u$  values. As the logarithm of the  $K_a$  values increased in the course of the affinity maturation, the magnitudes of the corresponding  $\Delta H$ ,  $\Delta C_p$ , and  $\Delta S_u$  values increased almost linearly. Although the interactions between a series of monoclonal antibodies and their same antigen have been investigated in several cases,<sup>35-37,39,43-45)</sup> the linear relationship between  $\log K_a$  and each of  $\Delta H$ ,  $\Delta C_p$ , and  $\Delta S_u$  shown in the present study has not been observed yet. On the basis of this correlation of the thermodynamic data along with the previously reported nuclear magnetic resonance (NMR) data,<sup>46)</sup> the mechanism of the affinity maturation will be discussed.

## 2. Materials and Methods

### 2.1 Chemicals

4-Hydroxy-3-nitrophenylacetic acid was purchased

from Sigma Chemical Co. 4-Hydroxy-3-nitrophenylacetyl caproic acid (NP-Cap) was synthesized from 4-Hydroxy-3-nitrophenylacetic acid and  $\epsilon$ -amino-n-caproic acid. All other chemicals were of reagent grade and used without further purification.

### 2.2 Preparation of Fab fragments

Anti-NP mouse monoclonal IgG antibodies, N1G9, 3B44, and 3B62, were purified from C57BL/6 mice hybridoma cell lines kindly provided by Professor K. Rajewsky, as described previously.<sup>46)</sup> The Fab fragments of these antibodies were prepared by papain digestion according to the procedure described previously.<sup>47)</sup> For brevity, the Fab fragments derived from N1G9, 3B44, and 3B62 will be designated as Fab (N1G9), Fab (3B44), and Fab (3B62), respectively.

### 2.3 Concentration determination

The concentration of NP-Cap was determined at 430 nm with use of the molar absorption coefficient,  $4230 \text{ M}^{-1} \text{ cm}^{-1}$ . The concentration  $1 \text{ mg ml}^{-1}$  of the Fab solution is equivalent to the absorbance at 280 nm, 1.73 (N1G9 and 3B62) and 1.57 (3B44).

### 2.4 Isothermal titration calorimetry (ITC)

Isothermal titration experiments were carried out on a Microcal OMEGA or MCS calorimeter interfaced with a microcomputer.<sup>18)</sup> The Fab solution was prepared by extensive dialysis against the experimental buffer, and the antigen was dissolved in the same dialysis buffer. The antigen solution was injected 20 times in  $5 \mu\text{l}$  increments and 3 min intervals into the Fab solution. The heat for each injection was subtracted by the heat of dilution of the injectant, which was measured by injecting the antigen solution into the dialysis buffer. Each corrected heat was divided by the moles of NP-Cap injected, and analyzed with Microcal Origin software supplied by the manufacturer.

## 3. Results

### 3.1 Determination of thermodynamic parameters

**Fig.1(a)** shows a typical ITC profile for the interaction between NP-Cap and Fab (3B62) at  $30.0^\circ\text{C}$ . An exothermic heat pulse was observed after each injection of NP-Cap into Fab (3B62). The magnitude of each peak decreased gradually with each new injection, and a small exothermic peak was still observed at a molar ratio of  $[\text{NP-Cap}]/[\text{Fab (3B62)}] = 2$ . The area of this exothermic peak was equivalent to the heat of dilution

An Isothermal Titration Calorimetric Study of The Antigen-Antibody Interaction:  
The Affinity Maturation of Anti-4-Hydroxy-3-Nitrophenylacetyl Mouse Monoclonal Antibody

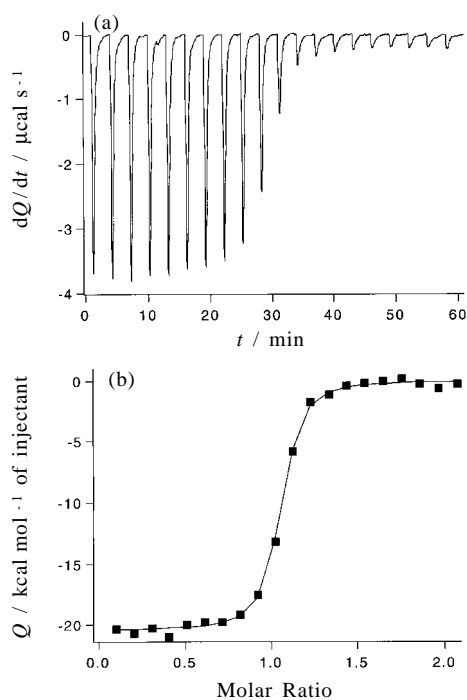


**Fig.1** Typical isothermal titration calorimetric profiles of the interaction between NP-Cap and Fab (3B62) at 30.0 °C. (a) The NP-Cap solution (1.0 mM in 5 mM sodium phosphate buffer, 200 mM sodium chloride, pH 8.0) was injected 20 times in 5  $\mu$ l increments into 38  $\mu$ M Fab (3B62) solution, which was dialyzed against the same buffer. Injections were occurred over 10 s at 3 min intervals. (b) Integrated areas for the above peaks were plotted against the molar ratio [NP-Cap]/[Fab (3B62)]. The data were fitted using a nonlinear least-squares method.

measured in a separate experiment by injection of NP-Cap into the buffer solution. The area under each peak was integrated, and the heat of dilution of NP-Cap was subtracted from the integrated values. The corrected heat was divided by the moles of NP-Cap injected, and the resulting values were plotted as a function of the molar ratio of [NP-Cap]/[Fab (3B62)], as shown in **Fig.1(b)**. The resultant titration plot was fitted to a sigmoidal curve using a nonlinear least-squares method. The binding constant,  $K_a$ , and the enthalpy change,  $\Delta H$ , were obtained from the fitted curve. Further, the Gibbs free energy change,  $\Delta G$ , and the entropy change,  $\Delta S$ , were calculated from the equation,  $\Delta G = -RT \ln K_a = \Delta H - T\Delta S$ .

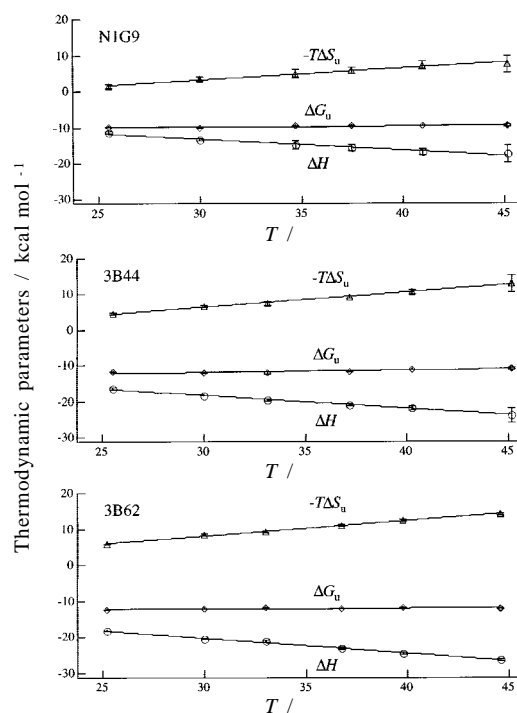


**Fig.2** Thermodynamic parameters [ $\Delta H$  (□),  $\Delta G_u$  (○), and  $-T\Delta S_u$  (△)] for the associations between NP-Cap and each of Fab (N1G9), Fab (3B44), and Fab (3B62) as a function of temperature. All experiments were performed in 5 mM sodium phosphate buffer, 200 mM sodium chloride, pH 8.0 at the experimental temperature. The solid lines were obtained from a linear least-squares regression.  $\Delta C_p$  was calculated from the slope of the regression line of  $\Delta H$  (□).

The magnitudes of the  $\Delta S$  and  $\Delta G$  values are dependent on the concentration units for the standard state. To obtain unitary entropy change,  $\Delta S_u$ , and unitary Gibbs free energy change,  $\Delta G_u$ , which are independent of the concentration units chosen for the standard state since, in essence, solute concentrations are measured in mole fraction units, the following equations were used<sup>48)</sup>:

$$\Delta S_u = \Delta S - R \ln X = \Delta S + 7.98 \text{ (cal mol}^{-1} \text{ K}^{-1})$$

$$\Delta G_u = \Delta G - 7.98 \times 10^{-3} T \text{ (kcal mol}^{-1})$$

The cratic contribution to the entropy change,  $R \ln X$ , is  $R \ln(1/55.6) = -7.98 \text{ cal mol}^{-1} \text{ K}^{-1}$ , where 55.6 M is the concentration of water in dilute aqueous solution.<sup>13)</sup> The thermodynamic parameters for the interaction between NP-Cap and each of Fab (N1G9) and Fab (3B44) were

**Table 1** Temperature dependence of thermodynamic parameters.

Fab	$T$	$K_a$ $M^{-1}$	$\Delta G_u$ $kcal\ mol^{-1}$	$\Delta H$ $kcal\ mol^{-1}$	$\Delta S_u$ $cal\ mol^{-1}\ K^{-1}$	$\Delta C_p^a$ $cal\ mol^{-1}\ K^{-1}$
N1G9	25.5	$(2.9 \pm 0.4) \times 10^5$	$-9.8 \pm 0.1$	$-11.2 \pm 0.3$	$-4.6 \pm 1.5$	$-309 \pm 27$
	30.0	$(2.7 \pm 0.3) \times 10^5$	$-9.9 \pm 0.1$	$-13.4 \pm 0.4$	$-11.3 \pm 1.7$	
	34.7	$(1.2 \pm 0.2) \times 10^5$	$-9.6 \pm 0.1$	$-14.7 \pm 1.1$	$-16.5 \pm 3.8$	
	37.5	$(9.8 \pm 1.4) \times 10^4$	$-9.6 \pm 0.1$	$-15.4 \pm 0.8$	$-18.9 \pm 3.0$	
	41.0	$(9.0 \pm 1.2) \times 10^4$	$-9.6 \pm 0.1$	$-16.8 \pm 1.0$	$-23.0 \pm 3.5$	
	45.2	$(6.5 \pm 1.5) \times 10^4$	$-9.6 \pm 0.2$	$-17.3 \pm 2.2$	$-24.2 \pm 7.6$	
3B44	25.5	$(7.5 \pm 1.0) \times 10^6$	$-11.8 \pm 0.1$	$-16.5 \pm 0.2$	$-15.7 \pm 0.9$	$-363 \pm 12$
	30.0	$(6.4 \pm 0.8) \times 10^6$	$-11.9 \pm 0.1$	$-18.4 \pm 0.1$	$-21.7 \pm 0.7$	
	33.1	$(5.1 \pm 1.2) \times 10^6$	$-11.8 \pm 0.2$	$-19.5 \pm 0.4$	$-24.8 \pm 1.9$	
	37.2	$(2.8 \pm 0.3) \times 10^6$	$-11.6 \pm 0.1$	$-20.9 \pm 0.2$	$-30.0 \pm 1.0$	
	40.3	$(8.0 \pm 1.3) \times 10^5$	$-11.0 \pm 0.1$	$-21.7 \pm 0.5$	$-34.3 \pm 2.0$	
	45.2	$(4.2 \pm 2.7) \times 10^5$	$-10.7 \pm 0.7$	$-23.9 \pm 2.0$	$-41.3 \pm 8.2$	
3B62	25.2	$(2.0 \pm 0.1) \times 10^7$	$-12.3 \pm 0.1$	$-18.3 \pm 0.1$	$-19.9 \pm 0.2$	$-415 \pm 12$
	30.0	$(8.0 \pm 0.7) \times 10^6$	$-12.0 \pm 0.1$	$-20.3 \pm 0.1$	$-27.5 \pm 0.5$	
	33.0	$(6.0 \pm 0.8) \times 10^6$	$-11.9 \pm 0.1$	$-21.2 \pm 0.2$	$-30.2 \pm 0.9$	
	36.8	$(5.2 \pm 1.0) \times 10^6$	$-12.0 \pm 0.1$	$-23.1 \pm 0.3$	$-35.9 \pm 1.4$	
	39.8	$(3.5 \pm 0.3) \times 10^6$	$-11.9 \pm 0.1$	$-24.5 \pm 0.2$	$-40.3 \pm 0.8$	
	44.6	$(3.3 \pm 0.3) \times 10^6$	$-12.0 \pm 0.1$	$-26.2 \pm 0.2$	$-44.8 \pm 0.7$	

<sup>a</sup> $\Delta C_p$  was determined from the slope of the temperature dependence of  $\Delta H$  between 25 and 45 °C.

obtained in the same way.

### 3.2 Temperature dependence of the antigen-antibody interaction

As a function of temperature between 25 °C and 45 °C, the interaction between NP-Cap and each of Fab (N1G9), Fab (3B44), and Fab (3B62) was analyzed by ITC. The thermodynamic parameters for these interactions are summarized in **Table 1**. The thermodynamic parameters,  $\Delta G_u$ ,  $\Delta H$ , and  $-T\Delta S_u$  are plotted as a function of temperature in **Fig.2**. For all of these interactions, both the  $\Delta H$  and  $\Delta S_u$  values were negative and exhibited strong temperature dependencies. By contrast, the negative  $\Delta G_u$  values showed only a weak dependency on temperature. Since the temperature dependencies of  $\Delta H$  and  $-T\Delta S_u$  had the opposite signs, their contributions to the temperature dependence of  $\Delta G_u$  were almost canceled out. The enthalpy-entropy compensation has been observed previously for other antigen-antibody interactions.<sup>41,44,45)</sup>

The associations between NP-Cap and the three anti-NP Fab were mainly driven by favorable negative changes in  $\Delta H$ . The negative  $\Delta H$  values decreased with increasing temperature, and showed linear dependence on temperature in the range of 25 ~ 45 °C (**Fig.2**). The  $\Delta C_p$  value for each interaction can be determined from

the slope of the temperature dependence of  $\Delta H$ . The negative  $\Delta C_p$  values of  $-309 \pm 27$ ,  $-363 \pm 12$ , and  $-415 \pm 12\ cal\ mol^{-1}\ K^{-1}$  were observed for Fab (N1G9), Fab (3B44), and Fab (3B62), respectively (**Table 1**).

**Fig.3** shows that the  $K_a$  values for NP-Cap correlate with each of the  $\Delta H$ ,  $\Delta C_p$ , and  $\Delta S_u$  values. As the logarithm of the  $K_a$  values increased in the order of Fab (N1G9), Fab (3B44), and Fab (3B62), the magnitudes of the corresponding  $\Delta H$ ,  $\Delta C_p$ , and  $\Delta S_u$  values increased almost linearly.

### 3.3 Ionic strength dependence of the antigen-antibody interaction

Existence of positively charged amino acid residues was suggested in the combining site of anti-NP Fab fragments.<sup>49)</sup> To analyze the electrostatic effect, the interaction between NP-Cap and each of Fab (N1G9), Fab (3B44), and Fab (3B62) was investigated by ITC as a function of the sodium chloride concentration between 20 mM and 400 mM. As the logarithm of the sodium chloride concentration increased, the logarithm of the  $K_a$  values of Fab (N1G9), Fab (3B44), and Fab (3B62) for NP-Cap decreased linearly as shown in **Fig.4**. The slopes of the regression lines in **Fig.4** were  $-0.57 \pm 0.09$ ,  $-0.59 \pm 0.10$ , and  $-0.48 \pm 0.07$  for Fab (N1G9), Fab (3B44), and Fab (3B62), respectively. Thus, the

An Isothermal Titration Calorimetric Study of The Antigen-Antibody Interaction:  
The Affinity Maturation of Anti-4-Hydroxy-3-Nitrophenylacetyl Mouse Monoclonal Antibody

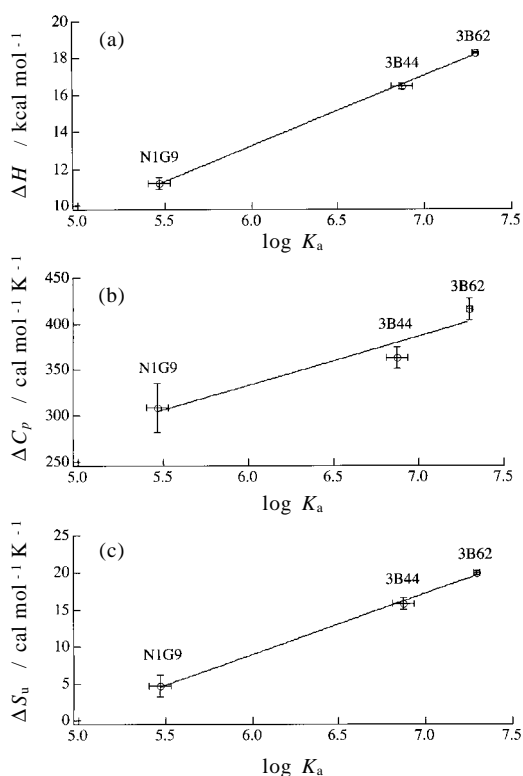


**Fig.3** Correlations between the  $K_a$  values at 25 °C and each absolute value of  $\Delta H$  at 25 °C (a),  $\Delta C_p$  (b), and  $\Delta S_u$  at 25 °C (c).

dependency of the  $K_a$  values of Fab (N1G9), Fab (3B44), and Fab (3B62) on the sodium chloride concentration was similar within experimental errors.

#### 4. Discussion

In the present study, the ITC analyses of the antigen-antibody associations in the affinity maturation were carried out to understand the mechanism of the affinity maturation. The present results revealed that all of the associations between NP-Cap and the three Fab were mainly driven by favorable negative changes in  $\Delta H$ . Van der Waals interactions and hydrogen bondings are usually considered to be the major potential sources of the negative  $\Delta H$  values.<sup>40,43,50</sup> Thus, it is suggested that van der Waals interactions and hydrogen bondings play a fundamental role in the interactions between NP-Cap and the three Fab. Also, the increase in the magnitude of the negative  $\Delta H$  with the increase in  $\log K_a$  (Fig.3(a)) suggests that, in the course of the affinity

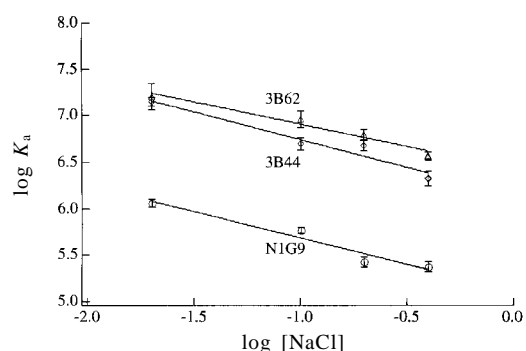


**Fig.4** Dependence of the  $K_a$  values of Fab (N1G9) (○), Fab (3B44) (□), and Fab (3B62) (△) for NP-Cap upon the sodium chloride concentration at 30 °C. All experiments were performed in 5 mM sodium phosphate buffer (pH 8.0) containing the experimental concentration of sodium chloride.

maturation, the increase in the van der Waals interactions and hydrogen bondings promotes the increase in the binding affinity of the anti-NP antibody.

The negative  $\Delta C_p$  values in **Table 1** are within the range of -100 to -650  $\text{cal mol}^{-1} \text{K}^{-1}$ , which were previously reported for various antigen-antibody associations.<sup>28,29,35,37,38,40,41,43-45</sup> In general, the negative  $\Delta C_p$  values for protein folding and protein-ligand association are proportional to the reduction in water-accessible nonpolar surface areas of the molecules, and related to the contribution of hydrophobic effect to molecular association.<sup>13-16,51</sup> To interpret the data quantitatively, the empirical method of Sturtevant<sup>52</sup> was used to estimate the hydrophobic and intramolecular vibrational contribution to  $\Delta C_p$  (**Table 2**). For all the three Fab, the calculated hydrophobic contribution to  $\Delta C_p$  was larger than the calculated vibrational contribution. Therefore, it is suggested that the observed negative change in  $\Delta C_p$  may primarily result from the hydrophobic effect, that is, the decrease in solvent exposure of both the aromatic antigen and the nonpolar groups in the binding site of the three Fab caused by the antigen-antibody association. Furthermore, the increase in the magnitude of the negative  $\Delta C_p$  with the increase in  $\log K_a$  (Fig.3(b)) suggests that, in the course of the affinity maturation, the increase in the hydrophobic effect contributes to the increase in the binding affinity of the anti-NP antibody. This is consistent with the previous

**Table 2** Hydrophobic and vibrational contributions to thermodynamic parameters at 25 °C.

Fab	hydrophobic components				vibrational components			
	$\Delta G_u$ kcal mol <sup>-1</sup>	$\Delta H$ kcal mol <sup>-1</sup>	$\Delta S_u$ cal mol <sup>-1</sup> K <sup>-1</sup>	$\Delta C_p$ cal mol <sup>-1</sup> K <sup>-1</sup>	$\Delta G_u$ kcal mol <sup>-1</sup>	$\Delta H$ kcal mol <sup>-1</sup>	$\Delta S_u$ cal mol <sup>-1</sup> K <sup>-1</sup>	$\Delta C_p$ cal mol <sup>-1</sup> K <sup>-1</sup>
N1G9	- 19.9	- 1.0	63.4	- 244	10.0	- 10.2	- 68.0	- 64.8
3B44	- 24.8	- 3.2	72.5	- 279	13.0	- 13.3	- 88.3	- 84.1
3B62	- 27.5	- 2.9	82.6	- 318	15.1	- 15.4	- 102.5	- 97.6

<sup>a</sup>All values were calculated by the empirical method of Sturtevant,<sup>52)</sup> using the thermodynamic data listed in Table 1.

NMR result that the binding site of NP-Cap was located in a similar position, but the combining site of Fab (3B62) with higher affinity for NP-Cap was composed of more Tyr residues than that of Fab (N1G9) with lower affinity for NP-Cap.<sup>46)</sup>

The hydrophobic effect, which drives the association of nonpolar surfaces of molecules by excluding water from the interface, would contribute to the positive change in  $\Delta S_u$ . However, the unfavorable negative  $\Delta S_u$  values were observed in the range of 25 ~ 45 , as shown in **Table 1**. Negative  $\Delta S_u$  has been observed previously for other antigen-antibody interactions.<sup>29-32,35,36,39-44)</sup> Consequently, it is concluded that some other factors should counteract the hydrophobic effect and make larger contributions to the negative  $\Delta S_u$ . Such effect to the negative  $\Delta S_u$  can be produced by the following factors; the constraint of intramolecular vibrational flexibility of Fab due to the antigen binding,<sup>52)</sup> the reduction in the translational and overall rotational degrees of freedom upon the complex formation,<sup>53,54)</sup> the conformational freezing of the amino acid residues of Fab caused by the antigen binding.<sup>55)</sup> The previously reported estimate of the factor was almost constant for different antigen-antibody complexes ( $T\Delta S_{TR} = 7 - 11$  kcal mol<sup>-1</sup>, where  $\Delta S_{TR}$  is an amount of translational and overall rotational entropy change).<sup>53-55)</sup> The estimation of the factor was previously reported in the interactions between lysozyme and a few anti-lysozyme monoclonal antibodies.<sup>55)</sup> The empirical method of Sturtevant<sup>52)</sup> was applied to estimate the hydrophobic and intramolecular vibrational (described above as the factor ) contribution to  $\Delta S_u$  (**Table 2**). For all the three Fab, the sign of the calculated hydrophobic contribution was positive, but that of the calculated vibrational contribution was indeed negative.

The obtained  $K_a$  values shown in **Table 1** increase

in the order of Fab (N1G9), Fab (3B44), and Fab (3B62), which was consistent with the previously reported results.<sup>2,4,5)</sup> As the logarithm of the sodium chloride concentration increased, the logarithm of the  $K_a$  values of the three Fab for NP-Cap decreased linearly. The dependency of the  $K_a$  values on the sodium chloride concentration was similar for the three Fab (**Fig.4**). These results suggest that the electrostatic effect is involved in the antigen-antibody associations, but the proportion of the electrostatic effect to the NP-Cap binding is similar for the three Fab. It is concluded that, in the course of the affinity maturation, the electrostatic effect does not significantly contribute to the increase in the binding affinity of the anti-NP antibody.

A linear correlation between  $\log K_a$  and each of  $\Delta H$ ,  $\Delta C_p$ , and  $\Delta S_u$  was found as shown in **Fig.3**. As the logarithm of the  $K_a$  values increased in the course of the affinity maturation, the magnitudes of the corresponding  $\Delta H$ ,  $\Delta C_p$ , and  $\Delta S_u$  values increased almost linearly. Although the interactions between a series of monoclonal antibodies and their same antigen have been investigated in several cases,<sup>35-37,39,43-45)</sup> the linear relationship between  $\log K_a$  and each of  $\Delta H$ ,  $\Delta C_p$ , and  $\Delta S_u$  shown in the present study has not been observed yet.

This linear relation of  $\log K_a$ ,  $\Delta H$ , and  $\Delta C_p$  (**Figs. 3(a) and 3(b)**) implies that the surface complementarity of the anti-NP antibody with the antigen increases in the course of the affinity maturation, which may reflect increased van der Waals interactions and hydrogen bondings between specific functional groups, and increased hydrophobic interactions with more exclusion of water molecules from the interface. However, the constancy of the electrostatic effect in the course of the affinity maturation (**Fig.4**) suggests that the number of electrostatic interactions involved in the interface remains unchanged with the increase in the surface complementarity. On the

other hand, more pronounced effect of unfavorable negative  $\Delta S_u$  was observed in the course of the affinity maturation (Fig.3(c)). This apparently contradicting effect seems feasible, because more enhanced surface complementarity would make more restraint in the intramolecular vibrations of the complex.

It is concluded that, in the course of the affinity maturation of the anti-NP antibody, a better surface complementarity is attained in the specific complex to obtain a higher binding affinity. The attainment of a better surface complementarity may be produced by an increase in the number of Tyr side chains in the antibody combining site.

### 5. Acknowledgments

This work was done in collaboration with Dr. T. Nakayama, Ms. M. Imazato, Prof. I. Shimada and Prof. Y. Arata (Faculty of Pharmaceutical Sciences, University of Tokyo), and Dr. A. Sarai (Tsukuba Life Science Center, The Institute of Physical and Chemical Research (RIKEN)). I thank Prof. K. Rajewsky (Institut für Genetik der Universität zu Köln) for generously providing the anti-NP mouse monoclonal antibody N1G9, 3B44, and 3B62 cell lines.

### References

- 1) G. W. Siskind and B. Benacerraf, *Adv. Immunol.* **10**, 1-50 (1969).
- 2) A. L. M. Bothwell, M. Paskind, M. Reth, T. Imanishi-Kari, K. Rajewsky, and D. Baltimore, *Cell* **24**, 625-637 (1981).
- 3) A. L. M. Bothwell, M. Paskind, M. Reth, T. Imanishi-Kari, K. Rajewsky, and D. Baltimore, *Nature* **298**, 380-382 (1982).
- 4) A. Cumano and K. Rajewsky, *Eur. J. Immunol.* **15**, 512-520 (1985).
- 5) A. Cumano, and K. Rajewsky, *EMBO J.* **5**, 2459-2468 (1986).
- 6) L. Wysocki, T. Manser, and M. L. Gefter, *Proc. Natl. Acad. Sci. U. S. A.* **83**, 1847-1851 (1986).
- 7) S. Crews, J. Griffin, H. Huang, K. Calame, and L. Hood, *Cell* **25**, 59-66 (1981).
- 8) C. Berek and C. Milstein, *Immunol. Rev.* **96**, 23-41 (1987).
- 9) R. S. Jack, T. Imanishi-Kari, and K. Rajewsky, *Eur. J. Immunol.* **8**, 559-565 (1977).
- 10) O. Makela and K. Karjalainen, *Immunol. Rev.* **34**, 119-128 (1977).
- 11) D. Allen, A. Cumano, R. Dildrop, C. Kocks, K. Rajewsky, N. Rajewsky, J. Roes, F. Sablitzky, and M. Siekevitz, *Immunol. Res.* **96**, 5-22 (1987).
- 12) D. Allen, T. Simon, F. Sablitzky, K. Rajewsky, and A. Cumano, *EMBO J.* **7**, 1995-2001 (1988).
- 13) W. Kauzmann, *Adv. Protein Chem.* **14**, 1-63 (1959).
- 14) C. Tanford, *The Hydrophobic Effect, 2nd Ed.*, Wiley-Interscience, New York (1980).
- 15) J. R. Livingstone, R. S. Spolar, and M. T. Record, Jr. *Biochemistry* **30**, 4237-4244 (1991).
- 16) R. S. Spolar and M. T. Record Jr., *Science* **263**, 777-784 (1994).
- 17) N. Langerman and R. L. Biltonen, *Methods Enzymol.* **61**, 261-286 (1979).
- 18) T. Wiseman, S. Williston, J. F. Brandts, and L.-N. Lin, *Anal. Biochem.* **179**, 131-137 (1989).
- 19) R. J. Baugh and C. G. Trowbridge, *J. Biol. Chem.* **247**, 7498-7501 (1972).
- 20) H. Fukada, K. Takahashi, and J. M. Sturtevant, *Biochemistry* **24**, 5109-5115 (1985).
- 21) K. Takahashi and H. Fukada, *Biochemistry* **24**, 297-300 (1985).
- 22) M. Milos, J.-J. Schaer, M. Comte, and J. A. Cox, *J. Biol. Chem.* **263**, 9218-9222 (1988).
- 23) F. P. Schwarz, K. Puri, and A. Surolia, *J. Biol. Chem.* **266**, 24344-24350 (1991).
- 24) G. Bains, R. T. Lee, Y. C. Lee, and E. Freire, *Biochemistry* **31**, 12624-12628 (1992).
- 25) F. P. Schwarz, K. D. Puri, R. G. Bhat, and A. Surolia, *J. Biol. Chem.* **268**, 7668-7677 (1993).
- 26) P. R. Connelly, J. A. Thomson, M. J. Fitzgibbon, and F. J. Bruzzese, *Biochemistry* **32**, 5583-5590 (1993).
- 27) P. R. Connelly, R. A. Aldape, F. J. Bruzzese, S. P. Chambers, M. J. Fitzgibbon, M. A. Fleming, S. Itoh, D. J. Livingston, M. A. Navia, J. A. Thomson, and K. P. Wilson, *Proc. Natl. Acad. Sci. U. S. A.* **91**, 1964-1968 (1994).
- 28) B. G. Barisas, J. M. Sturtevant, and S. J. Singer, *Biochemistry* **10**, 2816-2821 (1971).
- 29) M. F. M. Johnston, B. G. Barisas, and J. M. Sturtevant, *Biochemistry* **13**, 390-396 (1974).
- 30) J. F. Halsey and R. L. Biltonen, *Biochemistry* **14**, 800-804 (1975).
- 31) J. F. Halsey, J. J. Cebra, and R. L. Biltonen, *Biochemistry* **14**, 5221-5224 (1975).
- 32) B. W. Sigurskjold, E. Altman, and D. R. Bundle, *Eur. J. Biochem.* **197**, 239-246 (1991).

- 33) B. W. Sigurskjold and D. R. Bundle, *J. Biol. Chem.* **267**, 8371-8376 (1992).
- 34) D. A. Brummell, V. P. Sharma, N. N. Anand, D. Bilous, G. Dubuc, J. Michniewicz, C. R. MacKenzie, J. Sadowska, B. W. Sigurskjold, B. Sinnott, N. M. Young, D. R. Bundle, and S. A. Narang, *Biochemistry* **32**, 1180-1187 (1993).
- 35) R. F. Kelley, M. P. O'Connell, P. Carter, L. Presta, C. Eigenbrot, M. Covarrubias, B. Snedecor, J. H. Bourell, and D. Vetterlein, *Biochemistry* **31**, 5434-5441 (1992).
- 36) W. Ito, Y. Iba, and Y. Kurosawa, *J. Biol. Chem.* **268**, 16639-16647 (1993).
- 37) R. F. Kelley and M. P. O'Connell, *Biochemistry* **32**, 6828-6835 (1993).
- 38) K. P. Murphy, D. Xie, K. C. Garcia, L. M. Amzel, and E. Freire, *Proteins: Struct. Funct. Genet.* **15**, 113-120 (1993).
- 39) D. Tello, F. A. Goldbaum, R. A. Mariuzza, X. Ysern, F. P. Schwarz, and R. J. Poljak, *Biochem. Soc. Trans.* **21**, 943-946 (1993).
- 40) T. N. Bhat, G. A. Bentley, G. Boulot, M. I. Greene, D. Tello, W. D. Acqua, H. Souchon, F. P. Schwarz, R. A. Mariuzza, and R. J. Poljak, *Proc. Natl. Acad. Sci. U. S. A.* **91**, 1089-1093 (1994).
- 41) K. A. Hibbits, D. S. Gill, and R. C. Willson, *Biochemistry* **33**, 3584-3590 (1994).
- 42) K. Tsumoto, Y. Ueda, K. Maenaka, K. Watanabe, K. Ogasahara, K. Yutani, and I. Kumagai, *J. Biol. Chem.* **269**, 28777-28782 (1994).
- 43) X. Ysern, B. A. Fields, T. N. Bhat, F. A. Goldbaum, W. D. Acqua, F. P. Schwarz, R. J. Poljak, and R. A. Mariuzza, *J. Mol. Biol.* **238**, 496-500 (1994).
- 44) F. P. Schwarz, D. Tello, F. A. Goldbaum, R. A. Mariuzza, and R. J. Poljak, *Eur. J. Biochem.* **228**, 388-394 (1995).
- 45) J. N. Herron, D. M. Kranz, D. M. Jameson, and E. W. Voss Jr., *Biochemistry* **25**, 4602-4609 (1986).
- 46) T. Nakayama, Y. Arata, and I. Shimada, *Biochemistry* **32**, 13961-13968 (1993).
- 47) K. Kato, C. Matsunaga, T. Igarashi, H. Kim, A. Odaka, I. Shimada, and Y. Arata, *Biochemistry* **30**, 270-278 (1991).
- 48) R. W. Gurney, *Ionic Processes in Solution*, p.89, McGraw-Hill, New York (1953).
- 49) T. Azuma, N. Sakato, and H. Fujio, *Mol. Immunol.* **24**, 287-296 (1987).
- 50) P. D. Ross and S. Subramanian, *Biochemistry* **20**, 3096-3102 (1981).
- 51) C. Chothia, *Nature* **248**, 338-339 (1974).
- 52) J. M. Sturtevant, *Proc. Natl. Acad. Sci. U. S. A.* **74**, 2236-2240 (1977).
- 53) M. I. Page and W. P. Jencks, *Proc. Natl. Acad. Sci. U. S. A.* **68**, 1678-1683 (1971).
- 54) W. P. Jencks, *Proc. Natl. Acad. Sci. U. S. A.* **78**, 4046-4050 (1981).
- 55) J. Novotny, R. E. Bruccoleri, and F. A. Saul, *Biochemistry* **28**, 4735-4749 (1989).

### 要 旨

免疫過程が進行すると共に抗体が免疫原に対してより高い親和性を獲得する affinity maturation と呼ばれる現象の分子機構を明らかにするために、抗原分子 4-ヒドロキシ-3-ニトロフェニルアセチルカプロン酸 (NP-Cap) と 3 種類の抗 NP 抗体 N1G9, 3B44, 3B62 の Fab 断片との抗原抗体反応を等温滴定型熱量計 (ITC) により解析した。これらの抗原抗体反応はすべて、負のエンタルピー変化によって駆動されることが明らかとなった。このエンタルピー変化は 25 ~ 45 °C の温度範囲で温度に対して直線的に減少し、負の熱容量変化を与えた。一連の抗原抗体反応の結合定数が共存する塩化ナトリウムのイオン強度に対してどのように依存するかを解析したところ、抗 NP 抗体の affinity maturation の過程において、静電的相互作用は結合親和性の増大に寄与しないことが明らかとなった。また、抗 NP 抗体の affinity maturation の過程において一連の抗原抗体反応の結合定数の対数が増大するにつれて、一連の抗原抗体反応のエンタルピー変化や熱容量変化やユニタリーエントロピー変化の絶対値がほぼ直線的に増大することが明らかとなった。抗 NP 抗体の affinity maturation の過程において、より高い結合親和性を獲得するために、抗原抗体複合体においてより良い結合表面相補性が達成されていくことが、この一連の直線関係より結論づけられた。

鳥越秀峰 Hidetaka Torigoe  
理化学研究所筑波研究所, Tsukuba Life Science Center, The Institute of Physical and Chemical Research (RIKEN), TEL. 0298-36-9082, FAX. 0298-36-9080, e-mail: torigoe @rtc.riken.go.jp  
研究テーマ: 蛋白質・核酸の高次構造・構造安定性・相互作用  
趣味: 将棋